AVERAGE SOUND RADIATION MODEL FOR ORTHOTROPIC CROSS LAMINATED TIMBER PLATES

Andrea Santoni[1], Stefan Schoenwald[2], Bart Van Damme[2], Hans-Martin Tröbs[2], Patrizio Fausti[1]

[1] Engineering Department, University of Ferrara, Ferrara, Italy
andrea.santoni@unife.it
patrizio.fausti@unife.it

[2] Laboratory for Acoustics and Noise Control, EMPA, Dübendorf, Switzerland
stefan.schoenwald@empa.ch
bart.vandamme@empa.ch
hansmartin.trobs@empa.ch

Abstract
Cross Laminated Timber (CLT) engineered solid wood panels, that consist of an odd number of layers of timber beams glued together orthogonally, have become increasingly popular in building construction over the last two decades. The material provides good structural properties and is cost-competitive compared for example to masonry and concrete. However, due to the low volume density and its relative high stiffness, it cannot count on its mass to provide the sufficient acoustic performance required in buildings. Therefore it is important to investigate its vibro-acoustic behavior in order to develop proper acoustic measures to improve these structures. In this paper, which is part of an extensive analysis on sound radiation from CLT plates, we present a numerical model to predict the average radiation efficiency for CLT plates. The model is based on the simple assumption of thin orthotropic plate behaviour. Unlike for homogeneous isotropic thin plates, CLT's apparent stiffness depends on the angle of wave propagation in the material as well as on frequency. This is mainly caused by the layered structure of CLT. In order to consider all these effects, the proposed radiation model uses measured bending wavenumbers as input data.

1 Introduction

Cross Laminated Timber (CLT) engineered solid wood panels, that consist of an odd number of layers of timber beams glued together orthogonally, have gained growing success in construction market over the last two decades. This kind of building elements provides good structural stability and fulfils safety requirements. Complete elements are prefabricated and just connected at the construction site, reducing costs and times. For all these reasons CLT became a valuable alternative to the traditional building methods such as concrete and masonry. However, due to the low volume density and its relative high stiffness, it cannot rely solely on its mass to provide sufficient sound insulation required in buildings. During the design process the sound insulation performance of these elements needs to be assessed for the particular application and often needs to be improved, therefore it is important to

investigate the vibro-acoustic behaviour in order to develop proper acoustic solutions. One of the most important parameters in sound transmission analysis is the radiation efficiency, which describes how the vibrating structure converts mechanical energy into sound waves propagating in the surrounding fluid. Several authors presented different radiation models, as a reliable alternative to FE and BEM formulations, in order to reduce the computational time. Using the wavenumber transform approach Maidanik presented a modal formulation to evaluate the radiation efficiency for an in-vacuo single mode of rectangular plates [1]. Price and Croker [2], Wallace [3] and Leppington [4] presented refined versions of Maidanik's modal formulation. However, in dealing with broadband excitation or with input data of statistical energy analysis (SEA) based models, it is more convenient to consider an average radiation efficiency. Leppington derived an integral asymptotic formulation to evaluate the average radiation efficiency of a homogeneous isotropic rectangular plate, instead of computing each single mode radiation [4, 5]. Davy recently developed a model to compute both the real and the imaginary part of the specific average radiation wave impedance of finite rectangular panels [6], to take into account the fluid loading effect. An extensive overview on the different approaches to predict the sound radiation was presented by Atalla and Nicolas [7]. Mejdi and Atalla developed a prediction model for the vibro-acoustic response of stiffened plates [8], while Legault analysed orthogonally ribbed plates [9]. Due to its layered substructure, CLT presents a natural orthotropy, which means that the elastic and dynamic properties, unlike for homogeneous isotropic elements, are direction dependent [10]. In this paper we present a numerical model to predict the average radiation efficiency for orthotropic rectangular CLT plates, which is part of an extensive analysis on sound radiation from cross laminated timber structures. The model is based on the work presented by Anderson and Bratos-Anderson in [11] for a thin carbonate laminated plate. The formulation is conveniently modified in order to allow for frequency dependent input data, i.e. to use the flexural wavenumbers experimentally evaluated, instead of the material elastic or stiffness properties. In the next paragraph the basic concepts of orthotropic plate theory and sound radiation efficiency are recalled. In paragraph 3 the implemented radiation model is described. Then the model is finally validated comparing the numerical results with the experimental data.

2 Background theory

2.1 Orthotropic plates

Orthotropic plates, which are often used in building construction and for many other applications, have different elastic properties in two mutually perpendicular directions. This orthogonal anisotropy can be due to the presence of ribs or stiffeners, or, as for CLT plates, it can be an intrinsic characteristic of the material itself or its components, in case of layered media.

The equation of motion of a thin orthotropic plate, lying in the x-y plane, with the principal directions aligned with the orthogonal axes, undergoing free flexural vibrations, can be derived using Kirchhoff's theory for small deflections:

$$D_x \frac{\partial^4 w}{\partial x^4} + 2B \frac{\partial^4 w}{\partial x^2 \partial y^2} + D_y \frac{\partial^4 w}{\partial y^4} = \rho h \frac{\partial^2 w}{\partial t^2} \tag{1}$$

The bending stiffness along the principal directions D_x and D_y and the effective torsional stiffness B are determined from the material elastic constants:

$$D_x = \frac{E_x}{12(1-\nu^2)}; \quad D_y = \frac{E_y}{12(1-\nu^2)}; \quad B = \frac{\nu_y D_x}{2} + \frac{\nu_x D_y}{2} + 2\frac{G_{xy}}{12}h^3 \approx \sqrt{D_x D_y} \tag{2}$$

2

assuming $\nu = \sqrt{\nu_x \nu_y}$, where ν_x and ν_y are the elastic constants corresponding to the structure configuration [12]. The approximation of the torsional stiffness is based on the assumption that the in-plane shear modulus is a function of the shear moduli along the principal directions and the Poisson's ratio:

$$G_{xy} = \frac{\sqrt{E_x E_y}}{2(1+\nu)} \tag{3}$$

For these kind of structures a direction dependent bending stiffness has to be considered. It can be evaluated, for each propagation angle θ, at a given angular frequency ω, as:

$$D(\omega,\theta) = D_x(\omega)\cos^4\theta + 2B(\omega)\cos^2\theta\sin^2\theta + D_y(\omega)\sin^4\theta \tag{4}$$

Alternatively, it can be derived from the direction dependent bending wavenumber using the expression:

$$D(\omega,\theta) = \frac{\omega^2 \rho h}{k_B^4(\omega,\theta)} \tag{5}$$

The plate wavenumber k_B can be expressed as a function of the bending wavenumbers along the principal directions, $k_{B,x}$ and $k_{B,y}$, applying a well-established orthotropic elliptic model [11]:

$$k_B(\omega,\theta) = \sqrt{\left(k_{B,x}\cos\theta\right)^2 + \left(k_{B,y}\sin\theta\right)^2} \tag{6}$$

2.2 Radiation efficiency

The radiation efficiency of a vibrating structure is defined as the ratio between the total sound power W actually radiated by a structure and the sound power that would be theoretically radiated by a piston source having same surface area S and vibrating with the same mean square velocity of the surface $\langle v^2 \rangle_{t,s}$. It is given in Equation (6) and further depends on the characteristic air impedance $\rho_0 c_0$ [13].

$$\sigma = \frac{W}{\rho_0 c_0 S \langle v^2 \rangle_{t,s}} \tag{7}$$

The sound power radiated from a vibrating structure is usually analysed in terms of resonant modes, the Rayleigh's integral allows to evaluate the far-filed sound radiation due to the modal vibration distribution. Although this integral does not admit an analytical solution, as already mentioned, different numerical formulations have been proposed by several authors. However, as the number of modes within the frequency bandwidth increases, it can be more convenient to directly derive the average radiation efficiency instead of considering radiation of each single mode. An asymptotic approach for the average radiation efficiency was proposed by Leppington [4, 5], assuming:

- a sufficiently high modal density and modal overlap over the entire frequency range, to treat the discrete mode distribution as a continuous function;
- only the resonant modes are responsible for the sound radiation;
- all the resonant modes are uncorrelated;

- equipartition of the modal energy: all the modes within the frequency bands have equal energy.

Three different formulations were developed for three frequency regions, defined with respect to the coincidence condition, that occurs when the bending wavenumber k_B equals the acoustic wavenumber k_0:

$\mu > 1 + \delta$: below the coincidence condition;

$\mu = 1 \pm \delta$: near the coincidence condition;

$\mu < 1 - \delta$: above the coincidence condition.

where the dimensionless wavenumber μ is given by the ratio between the plate and the acoustic wavenumber:

$$\mu = \frac{k_B}{k_0} \tag{8}$$

Above coincidence the plate bending wavenumber k_B fits always to the project trace wavenumber of a sound wave propagating away from the surface under a certain angle. Therefore sound is radiated in this region uniformly from the whole plate surface like in case of a piston source. Thus, radiation efficiency approaches unity well above the critical frequency. Below coincidence the wavelength of sound in air is much bigger than the flexural wavelength on the plate. Therefore air particles move parallel to the plate surface to compensate the oscillating areas with high and low pressure. In this regime sound is only radiated at discontinuities, like the plate edges, where the pressure change cannot be fully be compensated by the moving air. Radiation efficiency is therefore usually much smaller than unity in this frequency region. At coincidence, due to the match of the waves, sound is radiated very well, even more efficiently than by a piston source and hence radiation efficiency even exceeds unity.

For the complete set of equations for the radiation efficiency defined for each frequency region please refer to Leppington's original papers. In the following analysis the equations of a rectangular plate with simply – supported edges baffled in a plane rigid surface of infinite extent are used.

3 Radiation model

In building acoustics perfectly diffuse sound fields are usually assumed for both experimental purposes and prediction models, which matches well with the assumptions in Leppington's model outlined above. The frequency dependent quantities are commonly expressed in one-third octave bands, thus it is advantageous and convenient to determine the averaged radiation efficiency for the use in sound transmission analysis. The implemented model is based on the work presented by Anderson and Bratos-Anderson [11] for specially orthotropic plates, for which the principal directions are aligned with the plate edges. The average radiation efficiency for a thin orthotropic baffled plate, with simply supported boundary conditions, is given by:

$$\sigma_{ortho}(\omega) = \frac{S}{\pi^2 n_d} \int_0^{\pi/2} \sigma(\omega,\theta) k_B \frac{\partial k_B}{\partial \omega} d\theta \tag{9}$$

The direction-dependent radiation efficiency $\sigma(\omega,\theta)$ can be computed using Leppington's average formulations, implementing a code for a discrete number of angles: $0<\theta<\pi/2$. Due to the orthotropic behaviour, the coincidence condition depends on the propagation direction of the bending wave,

therefore for each angle θ, the limits, to identify the three regions, should be defined. However, Leppington did not provide information on how those limits should be determined. The coincidence, or critical, condition is met when $\mu = 1$. In the implemented code the radiation efficiency is computed over the entire frequency range for all the three formulations first. The intersection between the *below* and *near-coincidence* curves defines the lower limit of the *near-coincidence* region: $\mu = 1+\delta$. Analogously the intersection between the *near* and *above-coincidence* curves defines the higher limit $\mu = 1-\delta$. The direction dependent radiation efficiency is finally obtained combining the three curves in the respective ranges. In Figure 1 the radiation index , $L_\sigma = 10log\sigma$, for each investigated propagation angle, is given as function of frequency.

The rate of change of the plate wavenumber with the frequency can be easily determined from equation (6):

$$k_B \frac{\partial k_B}{\partial \omega} = \frac{\left(k_{B,x}\cos\theta\right)^2 + \left(k_{B,y}\sin\theta\right)^2}{2\omega} \qquad (10)$$

For a thin orthotropic plate the modal density n_d, that describes the number of modes per Hertz, is given by:

$$n_d = \frac{L_x L_y \sqrt{\rho h}}{2\pi} \int_0^{\pi/2} \sqrt{1/D(\omega,\theta)}\, d\theta \qquad (11)$$

It should be noted that, since the code was implemented for a discrete number of angles $0<\theta<\pi/2$, the integrals, over θ in the equations (9) and (11) are replaced by sums, reducing drastically the algorithm computational cost.
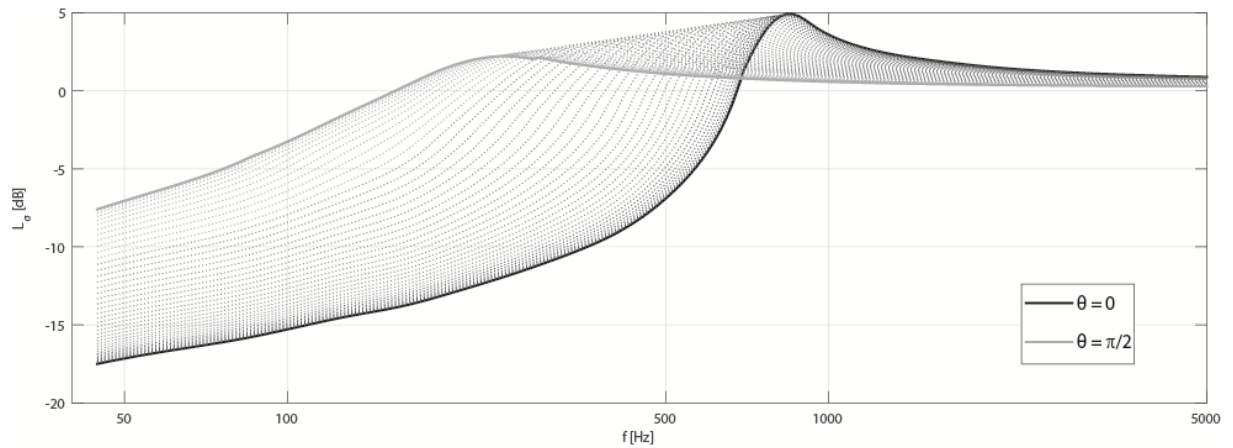
Figure 1 – Frequency dependent radiation index for different propagation angles $0 < \theta < \pi/2$.

4 Validation and results

The average radiation model was validated comparing the numerical results with the experimental data. The radiation efficiency was experimentally evaluated for a three-ply cross laminated timber plate with properties shown in Table 1. To perform the vibro-acoustic measurements the plate was

mounted into the rigid frame of Empa's wall sound insulation test facility. The vibration velocity was measured by a Polytec PSV-500 scanning laser vibrometer in a grid with 513 evenly distributed points that were approximately spaced 160 millimetres apart. A picture of the plate in the test condition is given in Figure 2.

Table 1 – Cross laminated timber plate geometric characteristics.

h [m]	L_x [m]	L_y [m]	ρ [kg/m^3]
0.08 – (0.03 + 0.02 + 0.03)	4.2	2.9	484.4

The plate was excited using an electrodynamic shaker, driven by a broadband white noise signal. The input impedance was obtained from the input force and the acceleration measured with a PCB 288D01 impedance head that was screwed into the wood and connected to the shaker with a stinger. Thus, it was also possible to evaluate the plate loss factor using the power injection method [14]. The radiation efficiency of the CLT plate was determined from the complex vibration velocity using the discrete calculation method (DCM) proposed by Hashimoto [15]. The experimental radiation efficiency was averaged over two different shaker positions to have a sufficient number of modes excited in the considered frequency range.

Figure 2 – Cross laminated timber plate installed in a rigid frame in Empa's wall sound insulation test facility

Table 2 – Plate flexural wavenumber along the principal directions and loss factor used as input data to evaluate the average radiation efficiency.

Frequency [Hz]	k_x [m^{-1}]	k_y [m^{-1}]	η [-]
50	3.29	1.68	0.08
63	3.70	1.89	0.08
80	4.19	2.15	0.08
100	4.68	2.40	0.08
125	5.23	2.69	0.08

160	5.99	3.08	0.07
200	6.70	3.46	0.07
250	7.51	3.88	0.07
315	8.50	4.41	0.06
400	9.72	5.06	0.05
500	10.97	5.74	0.04
630	12.51	6.59	0.03
800	14.44	7.67	0.03
1000	16.48	8.85	0.03
1250	18.91	10.28	0.03
1600	22.35	12.35	0.03
2000	25.99	14.62	0.03
2500	30.47	17.49	0.03
3150	36.31	21.28	0.03
4000	44.01	26.34	0.02
5000	52.99	32.33	0.02

The plate flexural wave velocity was experimentally determined, along the principal directions, for different frequencies. The measurement was performed similarly to the procedure presented by Nightingale [16] and it will be described in detail in a future paper. The bending wave velocity was measured using the time-of-arrival difference between two accelerometers. This was done for a series of narrowband pulses covering the entire frequency range. The results were then fitted with Mindlin's dispersion relation [17], Figure 3. The wavenumbers were directly determined from the experimental wave velocity. To account for the plate damping the measured loss factor is introduced into the plate wavenumber:

$$k_B^4 = {k_B^4}\Big/{(1 - j\eta)} \tag{12}$$

where k_B is determined from the wavenumber measured along the principal direction using the elliptic model equation (6) and j is the imaginary unit.

The experimental wavenumbers along the two principal directions are listed in one-third octave bands in Table 1 along with the measured loss factor. In the graph of Figure 4 the experimental average radiation index is plotted versus frequency together with the curves for each single shaker position. It is typical for orthotropic structures to be characterised by two distinct coincidence frequencies: the lowest one is associated with the stiffest plate principal direction, while the higher one is related to the orthogonal direction with a lower bending stiffness. The latter represents the critical condition: $\mu = 1$. The radiation efficiency peak around the critical condition falls in the frequency band centred around 800 Hz for the studied plate and due to the damping of the system is not very pronounced. Above this frequency the radiation efficiency tends asymptotically to unity. The lowest coincidence frequency, associated to the stiffest y-direction, falls in the 200 Hz frequency band. The region between the two coincidence frequencies exhibit a significantly greater sound radiation than an isotropic plate with only one coincidence frequency at 800 Hz.

The comparison between experimental and predicted radiation indexes is shown in Figure 5. The model provides a good approximation of the radiation trend. The predicted critical condition, as for the experimental curve, falls in the 800 Hz band, and has a sharper peak, even if the plate loss factor was taken into account. The coincidence frequency related to the stiffest direction is correctly located in the 200 Hz frequency band, even if it is not as accentuated as in the experimental results, but marked

by a change of the curve slope. The model is not able to approximate accurately the radiation efficiency below the critical frequency, where it is generally underestimated.
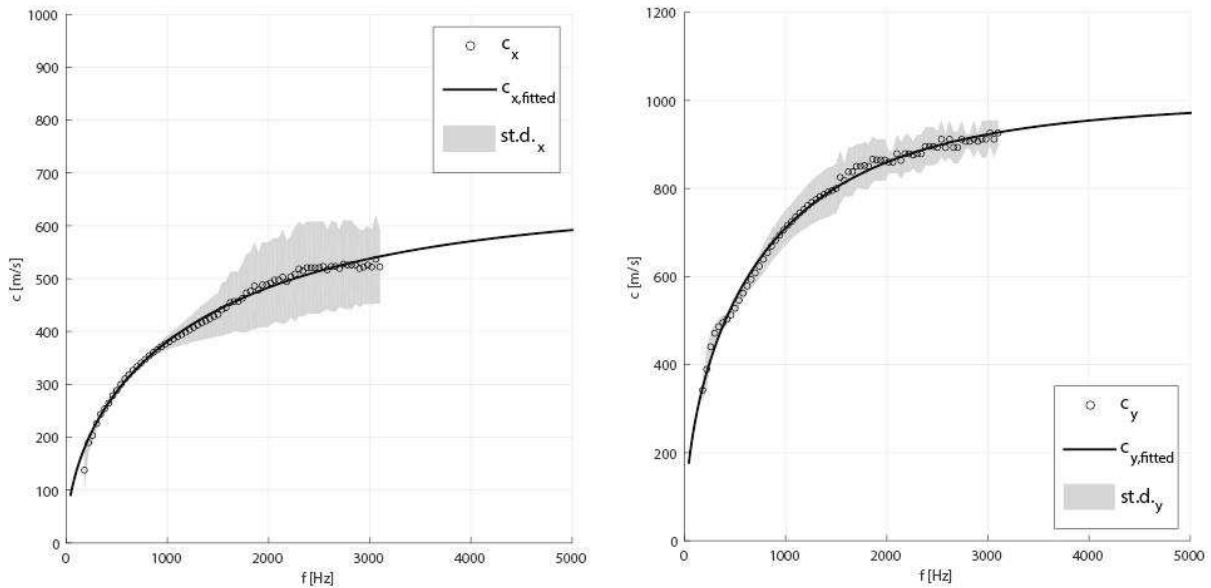
Figure 3 – Flexural wave velocity measured along the principal directions.
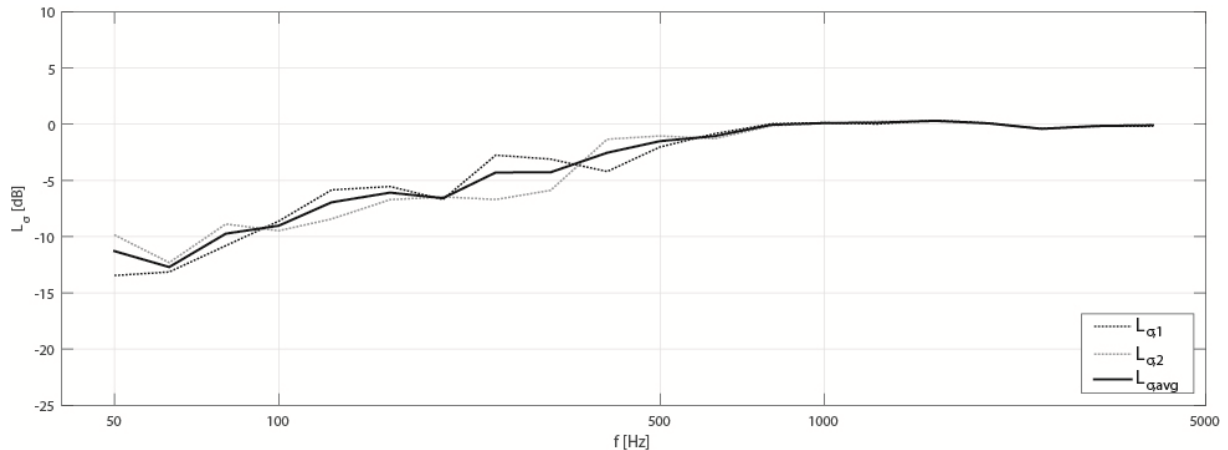
Figure 4 – Experimental radiation efficiency average over two source positions.

Reasons for this underestimation could be several effects that are not taken into account in the simplifying assumption made in the applied equations from Leppington. Below the upper coincidence frequency, sound is mainly radiated by discontinuities, like the plate boundaries. These are assumed to be simply supported in the model. In reality, the CLT plate is supported at its bottom edge by a frame whereas at all other edges there is a small gap, and the CLT is only connected to the rigid frame with elastic putty that is used to seal the gap and therefore might be able to move. This deviation from idealized boundary conditions, as well as the near flied around the excitation point, which represents another discontinuity that is not considered in the simple model, might enhance sound radiation and therefore could likely be the reason for the higher sound radiation in the experiment. Unfortunately, with the data and prediction model presented in this paper it is not possible to clearly explain the difference between predicted and measured results.
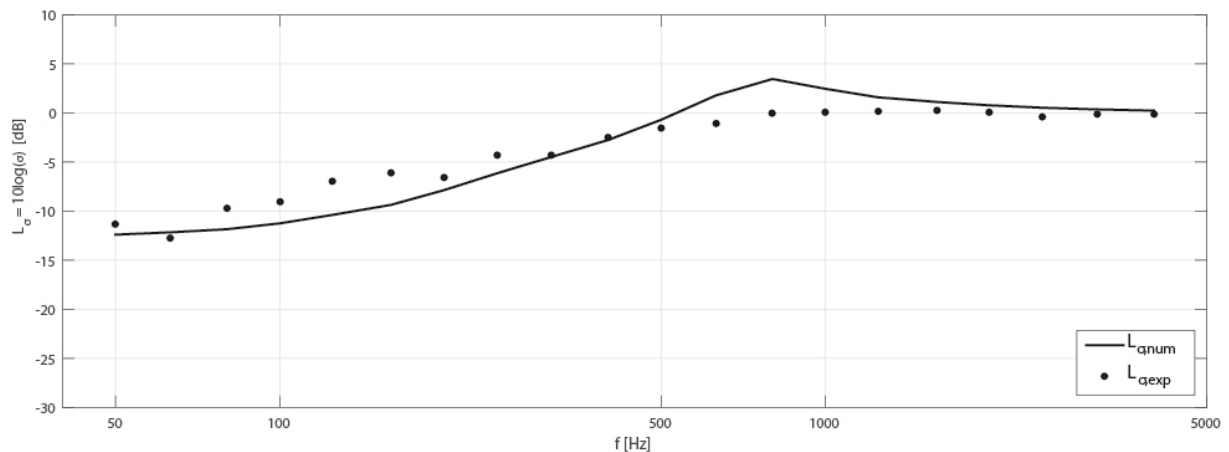
Figure 5 – Comparison between the experimental radiation index and the model result.

5   Conclusion

The radiation efficiency of a cross laminated timber building element has been numerically estimated using an asymptotic model developed for orthotropic plates. The model, assuming a high modal density over the entire frequency band, computes the plate radiation efficiency averaged over all the possible modes. The experimental flexural wavenumbers, measured along the principal directions, represent the model input data. The plate bending wavenumber for any propagation angle is approximated using an elliptical approach. The radiation efficiency of the CLT plate was experimentally evaluated from the complex velocity, measured on a 513 points grid, using the discrete calculation method. To validate the radiation model predicted results were compared with the experimental radiation efficiency. The model provides a good approximation of the radiation trend, evaluating accurately the critical frequency. The lowest coincidence frequency is also identified even if it is not as emphasized as in the experimental data. Below the critical condition the radiation efficiency is generally underestimated. Reasons could be the enhanced radiation due to boundary conditions at the plate edges that deviate in experiment from the ideal simply support assumed in the prediction and sound radiation at additional discontinuities in the experiment, like the nearfield of the excitation point, that are omitted in the prediction.

Although this model does not provide accurate information below the critical frequency, it is an useful tool during the design process, to perform a preliminary analysis of the sound radiation of building orthotropic elements in a very short time. The flexural wavenumbers, needed as input data, can be easily determined experimentally in laboratory as well as in situ, in real buildings, reducing some uncertainty caused by assumptions made for the elastic properties of the building elements. For more accurate analysis, more sophisticated models are needed but they are more time consuming and require a greater effort in the implementation.

9

References

[1] Maidanik, G. Response of ribbed panels to reverberant acoustic fields. *The Journal of the Acoustical Society of America*, 34(6), 1962, 809-826.

[2] Price, A. J.; M. J. Crocker. Sound transmission through double panels using statistical energy analysis. *The Journal of the Acoustical Society of America*, 47(3A), 1970, 683-693.

[3] Wallace, C. E. Radiation resistance of a rectangular panel. *The Journal of the Acoustical Society of America*, 51(3B), 1972, 946-952.

[4] Leppington F. G.; Broadbent E. G.; H. Heron K. The acoustic radiation efficiency of rectangular panels. *Proceedings of the Royal Society of London*, 382(1783), 1982, 245-271.

[5] Leppington F. G.; Broadbent E. G.; Heron K. H.; Mead S. M. Resonant and non-resonant acoustic properties of elastic panels. I. The radiation problem. *Proceedings of the Royal Society of London*, 406(1831), 1986, 139-171.

[6] Davy J. L. et al. The average specific forced radiation wave impedance of a finite rectangular panela). *The Journal of the Acoustical Society of America*, 136(2), 2014, 525-536.

[7] Atalla, N.; Nicolas J. A new tool for predicting rapidly and rigorously the radiation efficiency of plate like structures. *The Journal of the Acoustical Society of America*, 95(6), 1994, 3369-3378.

[8] Mejdi A.; Atalla N. Dynamic and acoustic response of bidirectionally stiffened plates with eccentric stiffeners subject to airborne and structure-borne excitations. Journal of Sound and Vibration, 329(21), 2010, 4422-4439.

[9] Legault, J.; Mejdi A.; Atalla N. Vibro-acoustic response of orthogonally stiffened panels: The effects of finite dimensions. *Journal of Sound and Vibration*, 330(24), 2011, 5928-5948.

[10] Van Damme B., Schoenwald S.; Alvarez Blanco M., Zemp A. Limitations to the use of Homogenized Material Parameters of Cross Laminated Timber Plates for Vibration and Sound Transmission Modelling, *Proceedings ICSV 22*, Florence, 2015, "In CD-ROM".

[11] Anderson, J. S.; Bratos-Anderson M. Radiation efficiency of rectangular orthotropic plates. *Acta acustic,a united with Acustica*, 91(1), 2005, 61-76.

[12] Szilard, R. *Theories and applications of plate analysis: classical numerical and engineering methods*. John Wiley & Sons, 2004.

[13] Fahy F. J.; Gardonio P. *Sound and structural vibration: radiation, transmission and response.* Academic press, 2007.

[14] Bloss B. C.; Rao M. D. Estimation of frequency-averaged loss factors by the power injection and the impulse response decay methods. *The Journal of the Acoustical Society of America*, 117(1), 2005, 240-249.

[15] Hashimoto, N. Measurement of sound radiation efficiency by the discrete calculation method. Applied Acoustics, 62(4), 2001, 429-446.

[16] Nightingale T. R. T.; Halliwell R.E.; Pernica G. Estimating in-situ material properties of a wood joist floor: Part 1–measurements of the real part of bending wavenumber. *Building Acoustics*, 11(3), 2004, 175-196.

[17] Graff, Karl F. *Wave motion in elastic solids*. Courier Corporation, 1975.